ACS Chemical Neuroscience
Cite This: ACS Chem. Neurosci. 2018, 9, 945−956
Research Article
pubs.acs.org/chemneuro

Matrix Metalloproteinase 9 Displays a Particular Time Response to Acute Stress: Variation in Its Levels and Activity Distribution in Rat Hippocampus

Felipe I. Aguayo,[†] Aníbal A. Pacheco,[†] Gonzalo J. García-Rojo,[†] Javier A. Pizarro-Bauerle,[†] Ana V. Doberti,[†] Macarena Tejos,[†] María A. García-Pérez,[†] Paulina S. Rojas,[‡] and Jenny L. Fiedler*[,†]

[†]Laboratorio de Neuroplasticidad y Neurogenética, Facultad de Ciencias Químicas y Farmacéuticas, Universidad de Chile, Santiago, Chile

[‡]Escuela de Química y Farmacia, Facultad de Medicina, Universidad Andres Bello, Santiago, Chile

Supporting Information

ABSTRACT: A single stress exposure facilitates memory formation through neuroplastic processes that reshape excitatory synapses in the hippocampus, probably requiring changes in extracellular matrix components. We tested the hypothesis that matrix metalloproteinase 9 (MMP-9), an enzyme that degrades components of extracellular matrix and synaptic proteins such as β-dystroglycan (β-DG_{43}), changes their activity and distribution in rat hippocampus during the acute stress response. After 2.5 h of restraint stress, we found (i) increased MMP-9 levels and potential activity in whole hippocampal extracts, accompanied by β-DG_{43} cleavage, and (ii) a significant enhancement of MMP-9 immunoreactivity in dendritic fields such as *stratum radiatum* and the molecular layer of hippocampus. After 24 h of stress, we found that (i) MMP-9 net activity rises at somatic field, i.e., *stratum pyramidale* and granule cell layers, and also at synaptic field, mainly *stratum radiatum* and the molecular layer of hippocampus, and (ii) hippocampal synaptoneurosome fractions are enriched with MMP-9, without variation of its potential enzymatic activity, in accordance with the constant level of cleaved β-DG_{43}. These findings indicate that stress triggers a peculiar timing response in the MMP-9 levels, net activity, and subcellular distribution in the hippocampus, suggesting its involvement in the processing of substrates during the stress response.

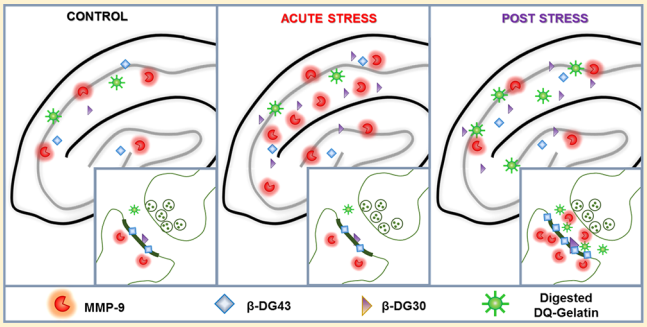

KEYWORDS: *Acute stress, Hippocampus, MMP-9, Synaptoneurosomes, β-Dystroglycan, Zymography*

INTRODUCTION

The ability of the brain to change and adapt in response to experience and a fluctuating environment is called neuroplasticity. This response involves synaptic remodeling, which includes formation and stabilization of new neural connections that enable important and complex processes, such as learning and memory consolidation.[1] The mechanisms that regulate neuroplasticity can be modulated through several factors. For instance, the stress response triggered by environmental challenges (either external or internal) produces a myriad of mediators that elicit well-orchestrated physiological modifications that may impact neuroplasticity processes. Stress induced by an emotional stressor activates the hypothalamic−pituitary−adrenal (HPA) axis, with a consequent release of adrenal glucocorticoids (cortisol in humans and corticosterone in rats), some of the stress hormones that target several limbic structures, such as the hippocampus.[2] This structure is implicated in the acquisition of episodic or declarative memory in humans and spatial memory in rodents.[3,4] Moreover, glucocorticoids trigger fast actions in the brain, promoting the release of glutamate from cortex and hippocampal areas,[5,6] accompanied by the subsequent activation of AMPA and NMDA receptors.[5−7] Interestingly, hippocampal formation negatively regulates HPA axis activity, evidencing their cross regulation.[8]

Acute stress seems to facilitate memory formation when the learning takes place in a stressful context[9] but usually impairs retrieval.[10] Probably, facilitation of memory formation involves neuroplastic processes that allow the reorganization of excitatory synapses, changing the balance between the formation and stabilization of dendritic spines that may sustain the functionality of neural circuits.[11] Several studies support the idea that synaptic remodeling requires dynamic changes in the expression of cell-surface adhesion molecules (reviewed in ref 12), as well as modifications in components of the extracellular matrix (ECM).[13] The ECM is a meshwork of proteins and proteoglycans in which proteolytic processing of its components supports a physiological mechanism to shape neuronal

Received: October 9, 2017
Accepted: January 23, 2018
Published: January 23, 2018

DOI: 10.1021/acschemneuro.7b00387
ACS Chem. Neurosci. 2018, 9, 945−956

circuits, such as those described in the hippocampus.[14] One set of degradative enzymes corresponds to matrix metalloproteinases (MMPs), which play a key role in both central nervous system (CNS) development and normal brain functioning.[15] Matrix metalloproteinase 9 (MMP-9) and its natural inhibitor, the tissue inhibitor of metalloproteinase 1 (TIMP-1), are expressed at low levels in the mature brain; nonetheless, they are induced in response to physiological and pathological conditions.[16−18] For instance, an increased level of MMP-9 expression has been detected in several brain areas, including the hippocampus, following fear conditioning.[19] Furthermore, studies have shown that both the expression and proteolytic activation of MMP-9 occur during the late phase of long-term potentiation (L-LTP) at CA3−CA1 synapses in the hippocampus.[20−22] Experiments with cortical primary cultures exposed to glutamate suggest that the signaling of glutamate receptors is required for the activation of MMP-9.[23] MMPs cleave a large number of substrates, including growth factors and precursors,[24] components of ECM such as laminin, and the chondroitin sulfate proteoglycan brevican,[25] the intercellular adhesion molecule I-CAM 5,[26] and the neural cell adhesion molecule N-cadherin,[27] among others.

Some *in vivo* exclusive substrates of MMPs have also been described in the brain. For instance, Nectin-3 corresponds to a cellular adhesion, Ig-like, transmembrane protein predominantly expressed postsynaptically.[28] In the hippocampus, Nectin-3 levels at synaptic sites are reduced by chronic stress; variations have been associated with an enhancement in the gelatinolytic activity of MMP-9.[29] From a functional point of view, the lower level of expression of Nectin-3 has been associated with alterations in cognitive function and social recognition.[29] Additionally, β-dystroglycan 43 (β-DG$_{43}$), which was first described as a substrate for MMP-2 and MMP-9 in an experimental model of autoimmune encephalopathy,[30] is also processed *in vivo* by MMP-9 in response to enhanced excitatory neurotransmission in the hippocampus.[23] β-DG$_{43}$ is a dual-function protein that acts as a signal transducer between the ECM and the cytoskeleton[31] and controls dendritic morphogenesis of hippocampal neurons *in vitro*.[32] Similarly, changes in MMP-9 activity play a key role in neuronal morphology by promoting the elongation of dendritic spines.[21,33] Importantly, in the hippocampus, β-DG$_{43}$ and MMP-9 are colocalized *in vivo* at the excitatory synapse.[23] Considering that stress influences glutamate neurotransmission[5,6] and promotes remodeling of the brain,[34] the aim of this study was to evaluate the consequences of acute stress on MMP-9 levels and activity in the hippocampus, variations that may be useful for understanding the mechanisms that transform an adaptive response into a maladaptive one.

RESULTS AND DISCUSSION

Physiological Parameters. Adult male rats were acutely stressed by motion restraint for 2.5 h. This stressor produces the activation of the HPA axis, inducing a fast secretion of corticotropin releasing hormone (CRH).[35] We evaluated the effectiveness of the restraint procedure by measuring fecal output, which is driven by CRH release in the brain.[36,37] A significant increase in the number of fecal pellets voided by stressed animals was observed during the 2.5 h of restraint in comparison to the number voided by unstressed animals (P < 0.0001) (Figure 1A). We also found that after this stress procedure, there was an almost 28-fold increment in corticosterone (CORT) levels in comparison to those of controls (P < 0.0001) (Figure 1B). Twenty-four hours after the acute stress session, CORT levels were higher than those of controls (P < 0.0368; 12-fold) but lower than those of stressed animals (P < 0.0086) (Figure 1B). Therefore, acute restraint stress activates the HPA axis, with the consequent increase in fecal pellet output and CORT release.

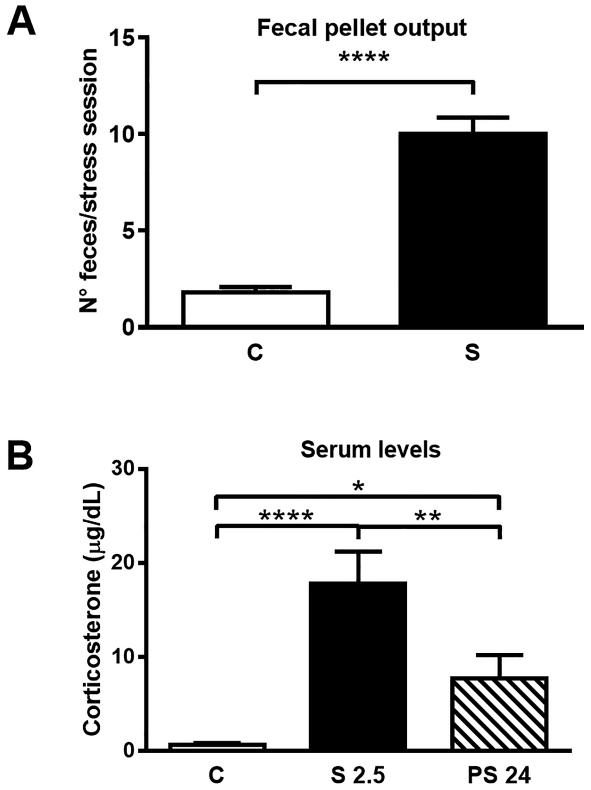

Figure 1. Effect of acute restraint stress on fecal pellet output and serum corticosterone levels. (A) The graph shows means ± the standard error of the mean (SEM) of the number of fecal pellets released by control unstressed rats and stressed rats with 2.5 h of restraint stress. Data were analyzed by a nonparametric one-tail Mann−Whitney test. (B) Acute restraint stress promotes an increase in serum corticosterone levels at the end of the stress session (S 2.5), returning to levels similar to that of the control 24 h poststress (PS 24). Data were analyzed with a nonparametric Kruskal−Wallis test (P < 0.0001), followed by Dunn's post hoc test. Control animals (C) were maintained in the home cage for 2.5 h (n = 12); stressed animals (S) were maintained in the home cage for 2.5 h (n = 36). Part of the stressed group was sacrificed immediately (S 2.5) (n = 16), and the rest of the animals were sacrificed 24 h poststress (PS 24) (n = 20). *P < 0.05; **P < 0.01; ****P < 0.0001.

Effect of Acute Stress on MMP-9, β-DG$_{43}$, TIMP-1, and MMP-2 Protein Levels. We investigated by Western blot whether acute stress promotes variation in levels of MMP-9, its substrate (β-DG$_{43}$), its enzymatic regulator (TIMP-1), and MMP-2. A representative blot of the whole hippocampal extract is shown in Figure 2A, and a rise in the level of MMP-9 was detected (Figure 2B). Nonparametric Kruskal−Wallis analysis indicated differences between groups (P = 0.0012), and Dunn's analysis indicated that during the stress procedure, there was a 50% increase in MMP-9 immunoreactivity in the whole hippocampal extract (P < 0.05) (Figure 2B). During the recovery period after stress (i.e., 24 h after the stress procedure), MMP-9 levels were reduced in comparison to those from the stress period (P < 0.01), reaching levels similar to that of the control group (Figure 2B). Interestingly, this

DOI: 10.1021/acschemneuro.7b00387
ACS Chem. Neurosci. 2018, 9, 945−956

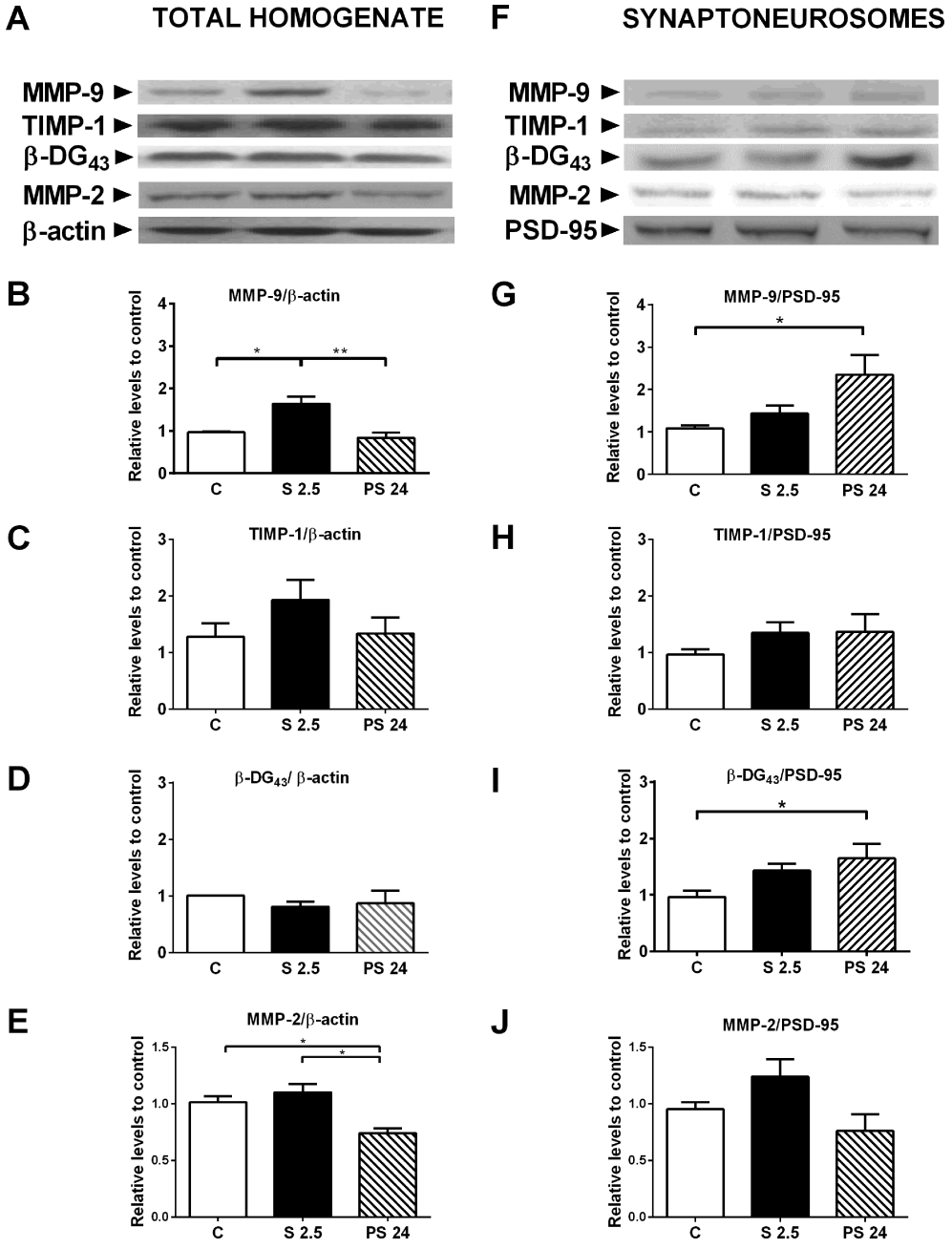

Figure 2. Effects of acute stress on levels of MMP-9, its natural inhibitor (TIMP-1), its substrate (β-DG$_{43}$), and MMP-2. (A) Representative immunoblots against MMP-9, TIMP-1, β-DG$_{43}$, and MMP-2. (B) Graph showing the ratio between MMP-9 and β-actin. Data were analyzed by a nonparametric Kruskal–Wallis test (P = 0.0012) followed by Dunn's post hoc test. Control (C) (n = 5), animals stressed for 2.5 h that were sacrificed immediately (S 2.5) (n = 5), and animals sacrificed 24 h poststress (PS 24) (n = 5). (C) Ratio between TIMP-1 and β-actin (C, n = 7; S 2.5, n = 5; PS 24, n = 4) and (D) β-DG$_{43}$ and β-actin (C, n = 4; S 2.5, n = 4; PS 24, n = 4). (E) Ratio between MMP-2 and β-actin. Data were analyzed by a nonparametric Kruskal–Wallis test (P = 0.0015) followed by Dunn's post hoc test (C, n = 6; S 2.5, n = 3; PS 24, n = 5). (F) Representative immunoblots against MMP-9, TIMP-1, β-DG$_{43}$, MMP-2, and PSD-95 in the synaptoneurosome fraction. (G) Graph showing the ratio between MMP-9 and PSD-95. Data were analyzed by a nonparametric Kruskal–Wallis test (P = 0.0133) followed by Dunn's post hoc test (C, n = 5; S 2.5, n = 3; PS 24, n = 6). (H) Ratio between TIMP-1 and PSD-95 (C, n = 6; S 2.5, n = 3; PS 24, n = 6). (I) Ratio between β-DG$_{43}$ and PSD-95. Data were analyzed by a nonparametric Kruskal–Wallis test (P = 0.0179) followed by Dunn's post hoc test (C, n = 6; S 2.5, n = 3; PS 24, n = 6). (J) Ratio between MMP-2 and PSD-95 (C, n = 6; S 2.5, n = 3; PS 24, n = 5). *P < 0.05; **P < 0.01.

increment in MMP-9 levels was not accompanied by changes in the levels of its natural negative regulator, TIMP-1 (Figure 2C), or its substrate, β-DG$_{43}$ (Figure 2D), either during or after the acute stress session. On the other hand, nonparametric Kruskal–Wallis analysis of MMP-2 levels indicated differences between groups (P = 0.0015), and Dunn's analysis indicated that levels of this enzyme were diminished 24 h after stress in comparison to those of the control (P = 0.0234) and stressed (P = 0.0335) (Figure 2E) groups.

To examine whether these changes occur at synaptic sites, we used a synaptoneurosome preparation that corresponds to a fraction enriched with dendritic excitatory spines.[38] Electron micrographs of this fraction showed enrichment in structures such as resealed axon terminals (containing vesicular

DOI: 10.1021/acschemneuro.7b00387
ACS Chem. Neurosci. 2018, 9, 945–956

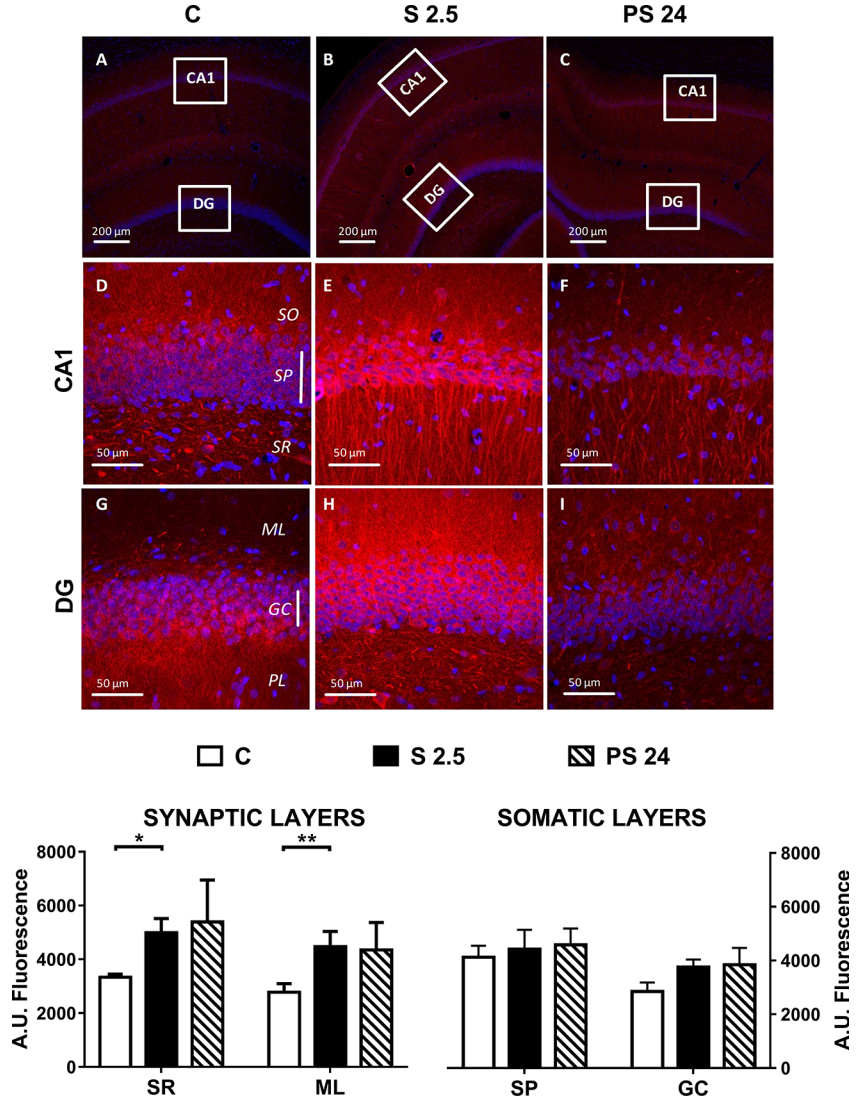

Figure 3. Effect of stress and recovery period on the MMP-9 immunoreactivity of hippocampal regions. (A–C) Representative confocal fluorescent photomicrographs showing MMP-9 (red fluorescence) and Hoechst-labeled nuclei (blue fluorescence), at 10× magnifications of rat hippocampus; 40× magnifications of CA1 (D–F) and DG (G–I) are also shown. The bottom panel displays a quantitative analysis, showing that acute restraint stress promotes an increment in MMP-9 immunofluorescence in the *stratum radiatum* of CA1 and the molecular layer of dentate gyrus (DG), returning to control levels 24 h poststress in both synaptic layers. On the other hand, MMP-9 immunofluorescence levels in both the *stratum pyramidale* and the granule cell layer were insensitive to stress and recovery period. Abbreviations: C, control animals; S 2.5, animals stressed for 2.5 h that were sacrificed immediately; PS 24, animals sacrificed 24 h poststress; DG, dentate gyrus; SO, *stratum oriens*; SP, *stratum pyramidale*; SR, *stratum radiatum*; ML, molecular layer; GC, granule cell layer; PL, polymorphic layer. Data were analyzed by a nonparametric Kruskal–Wallis test, followed by Dunn's post hoc test (C, $n = 7$; S 2.5, $n = 5$; PS 24, $n = 6$). *$P < 0.05$; **$P < 0.01$.

structures) associated with resealed postsynaptic compartments, which were characterized by a densely stained membrane and represented the postsynaptic density (see Figure S1A). Western blotting analysis did not detect immunoreactivity for the glial marker [glial fibrillary acidic protein (GFAP)] or the nuclear marker (LAP-2a) in the synaptoneurosome fraction (see Figure S1B). In contrast, this fraction was enriched with synaptophysin (a presynaptic marker) and PSD-95 (a postsynaptic marker) (see Figure S1B). Moreover, MMP-9 and MMP-2 were poorly detected in the nuclear fraction, and the nuclear fraction was enriched with both TIMP-1 and β-DG$_{43}$ (see Figure S1B). We then evaluated the effect of acute stress and recovery period on synaptoneurosome fraction protein levels using PSD-95 as a loading control (Figure 2F). Kruskal–Wallis analysis revealed significant differences in MMP-9 levels between groups ($P = 0.01$), and postanalysis showed no changes during the 2.5 h stress period. However, a significant increase of approximately 2.5-fold over the control value was observed 24 h poststress ($P < 0.05$) (Figure 2G), indicating synaptic sites were enriched with MMP-9 during the stress recovery period. Interestingly, TIMP-1 levels did not differ in comparison to those of unstressed animals (Figure 2H). In contrast, Kruskal–Wallis analysis ($P = 0.02$) and postanalysis revealed a significant ($P < 0.05$) enrichment with β-DG$_{43}$ (uncleaved form) at synaptic sites 24 h poststress (Figure 2I). In contrast to the total hippocampal extract, MMP-2 levels in the synaptoneurosome fraction were not modified by experimental conditions (Figure 2J).

MMP-9 is expressed in adult brain neurons of the cerebral cortex, cerebellum, and hippocampus.[39] Several investigations have demonstrated that MMP-9 gene expression, translation, and activity are tightly controlled. For instance, the MMP-9

DOI: 10.1021/acschemneuro.7b00387
ACS Chem. Neurosci. 2018, 9, 945–956

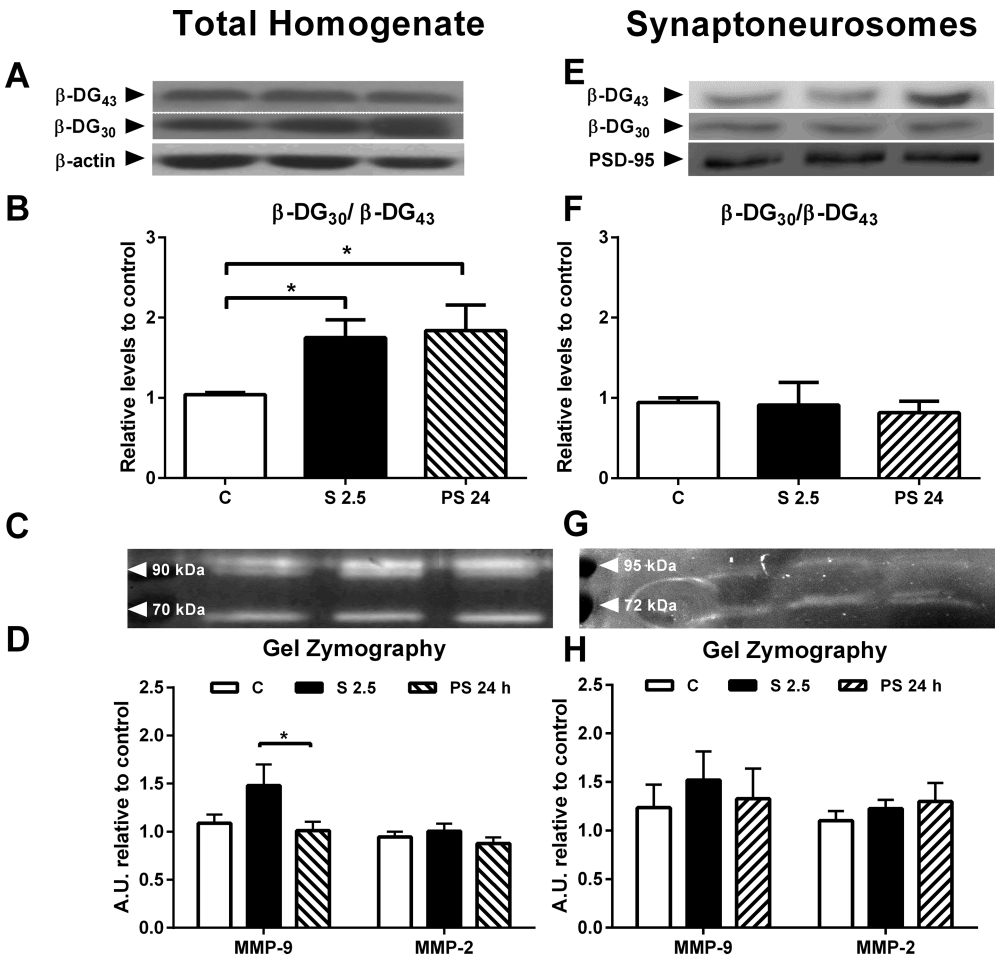

Figure 4. Stress promotes β-DG$_{43}$ cleavage, along with a rise in potential MMP-9 activity, but only in the total hippocampal homogenate. (A) Representative immunoblots against β-DG$_{30}$ and β-DG$_{43}$. (B) Graph showing the processed β-DG$_{30}$/β-DG$_{43}$ ratio. Data were analyzed by a nonparametric Kruskal–Wallis test (P = 0.0145), followed by Dunn's post hoc test (C, n = 4; S 2.5, n = 4; PS 24, n = 4). (C) Representative gelatin zymograph showing MMP-9 potential *in vitro* activity. (D) Graph showing the relative activity of MMP-9 in experimental groups. No variation was observed in MMP-2 activity. Data were analyzed by a nonparametric Kruskal–Wallis test (P = 0.0125), followed by Dunn's post hoc test (C, n = 4; S 2.5, n = 4; PS 24, n = 4). (E) Representative immunoblots against β-DG$_{43}$, β-DG$_{30}$, and PSD-95 of the synaptoneurosome fraction. (F) Graph showing the relative abundance of DG$_{30}$/β-DG$_{43}$ (C, n = 5; S 2.5, n = 3; PS 24, n = 4). (G) Representative gel zymograph showing MMP-9 activity. (H) Graph showing the relative activity of MMP-9, obtained from gelatin zymography. No variation was observed in MMP-2 activity (C, n = 3; S 2.5, n = 3; PS 24, n = 3). *P < 0.05.

gene is constitutively expressed in the brain but is also induced under conditions of enhanced excitatory neurotransmission, i.e., seizures[40] and LTP.[17,18] Furthermore, minutes after hippocampal LTP induction, MMP-9 mRNA dendritic transport is triggered,[16] accompanied by a fast translation and activation of this enzyme.[20] Transport of MMP-9 mRNA to dendrites triggered by neuronal activity involves the fragile X mental retardation protein (FMRP),[41] which acts as a translational repressor.[42] Because MMP-9 levels can be locally modulated by neuronal activity, we evaluated changes in MMP-9 immunoreactivity at hippocampal subfields. A global analysis at low magnification showed an increment in MMP-9 immunoreactivity after 2.5 h of stress, an effect not observed 24 h poststress (Figure 3A–C). Comparison at a higher magnification showed that stress increases MMP-9 immunoreactivity in the *stratum radiatum* of CA1 (compare panels D and E of Figure 3) and the molecular layer of dentate gyrus (compare panels G and H of Figure 3). Quantitative analysis indicated that stress induces an increase in immunoreactivity, almost 35 and 70% in the *stratum radiatum* of CA1 and the molecular layer, respectively (Figure 3, bottom panel). Twenty-four hours poststress, MMP-9 immunoreactivity at the *stratum radiatum* (compare panels D and F of Figure 3) and the molecular layer (panels G and I of Figure 3) seems to be slightly higher than control values; nonetheless, statistical analysis indicated no significant differences.

Both biochemical analysis and immunofluorescence approaches showed an increase in MMP-9 levels at 2.5 h of stress, an increment that was also observed in the synaptoneurosome fraction, but with a delay of 24 h after the stress procedure. The changes detected in the whole hippocampal extract along with those in synaptic layers may be driven by vesicular trafficking from the soma to the dendritic compartment. Indeed, in hippocampal cultured neurons, MMP-2- and MMP-9-containing vesicles are preferentially distributed in the somato-dendritic compartment and are also found within dendritic protrusions, supporting a mechanism by which MMPs can be secreted, to act extracellularly on their substrates.[43]

Effect of Acute Stress on MMP-9 Potential Activity. Next, we indirectly evaluated whether the increase in the level of MMP-9 is accompanied by changes in its activity, considering the proteolytic processing of β-DG$_{43}$ as a marker

DOI: 10.1021/acschemneuro.7b00387
ACS Chem. Neurosci. 2018, 9, 945–956

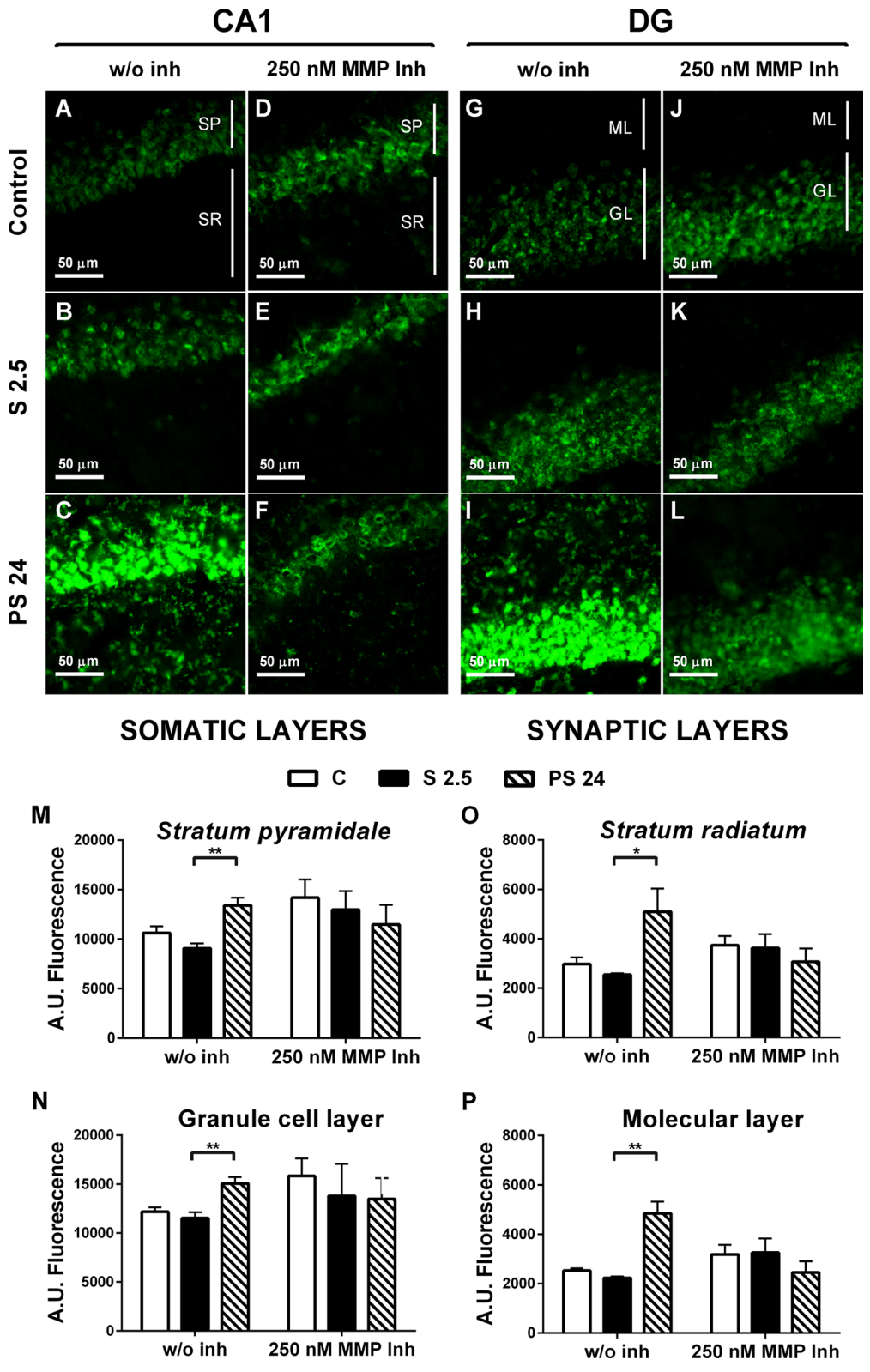

Figure 5. Effect of stress and recovery period on gelatinolytic activity detected by *in situ* zymography in the hippocampus and its sensitivity to the MMP inhibitor. Gelatinolytic activity appeared as green fluorescence produced after incubation of coronal brain sections (35 μm thick) with the fluorogenic substrate DQ gelatin. The images in panels A–C represent epifluorescent photomicrographs (without inhibitor, w/o inh) showing hippocampus subfields (C, n = 6; S 2.5, n = 5; PS 24, n = 5). To test whether gelatinolytic activity was related to MMP-9 activity, adjacent coronal slices were incubated prior to and during the incubation with DQ gelatin in the presence of 250 nM MMP inhibitor (MMP inh) (C, n = 6; S 2.5, n = 3; PS 24, n = 4). Abbreviations: SP, *stratum pyramidale*; SR, *stratum radiatum*; ML, molecular layer; GC, granule cell layer (scale bar, 50 μm). The bottom panel shows a quantitative analysis of fluorescence intensity, showing that the PS 24 procedure promotes an increment in gelatinase activity in the *stratum radiatum* of CA1 and the molecular layer of dentate gyrus, the pyramidal cell layer, and the granule cell layer. Data were analyzed by a nonparametric Kruskal–Wallis test, followed by Dunn's post hoc test. *P < 0.05; **P < 0.01.

DOI: 10.1021/acschemneuro.7b00387
ACS Chem. Neurosci. 2018, 9, 945–956

of *in vivo* enzyme activity.[23,30] To visualize uncleaved β-DG_{43} and cleaved product (30 kDa, β-DG_{30}), we exposed the Western blot short and long periods to obtain a linear signal response (Figure S2). In controls, we detected a 30 kDa immunoreactive band in whole hippocampal homogenates (Figure 4A), indicating baseline proteolytic processing of β-DG_{43}. Furthermore, stress produced a significant increase of almost 70% in the β-DG_{30}/β-DG_{43} ratio [Kruskal–Wallis P = 0.0145 (Figure 4B)], which was coincident with the increased MMP-9 levels (Figure 2B) and accumulation of β-DG_{30} form 24 h poststress (Figure 4B). We then used substrate gel zymography, which is a technique that reveals gelatinolytic activities and their molecular weights. In the case of MMP-2 and MMP-9, the technique detects the activities related to zymogens, activated forms, and those of the enzyme released from the binding of its TIMP.[44] Gel zymography performed with the total homogenate of hippocampus revealed five activities (Figure S3, lines 2–4 and gelatinolytic activities labeled as a–e) that migrated at molecular weights between 250 and 70 kDa, which have been described as MMP-9 activities found in human plasma.[45] The activity in rat serum around 70 and 90 kDa corresponded to MMP-2 and MMP-9, respectively (Figure S3, lines 5 and 6, respectively). In other biological samples, the gelatinolytic activity observed at 130 kDa has been associated with MMP-9 heterodimers that may contain NGAL[46] or TIMP-1.[47,48] On the other hand, the activities detected at a high molecular weight (>180 kDa) may correspond to multimeric forms of MMP-9.[49,50] We decided to evaluate the effect of stress and recovery period on the potential activity (i.e., zymogen; both active and those released from its inhibitor) of the MMP-9 monomer (near 90 kDa) and MMP-2 (near 70 kDa), because this information may be useful as a measure of enzyme levels. Figure 4C shows an increase in the potential activity of MMP-9 by stress, but not in that of MMP-2. Kruskal–Wallis analysis of MMP-9 data indicated significant differences among groups (P = 0.0125), and Dunn's post hoc test indicated an increment in MMP-9 potential activity in stressed animals in comparison to that seen during the recovery period (P = 0.0284) (Figure 4D), with no effect on MMP-2 potential activity (Figure 4D).

Our next step was to evaluate variation in the processing of β-DG_{43} in the synaptoneurosome fraction, given that synaptic membranes of sheep brain[51] and somatodendritic compartments in rodents[23,52,53] are enriched with this protein. We found that neither the β-DG_{30}/β-DG_{43} ratio (Figure 4F) nor the potential activity of MMP-9 and MMP-2 evaluated by gel zymography was modified by stress or the recovery period in synaptoneurosomes (Figure 4E,H). The differences in MMP-9 potential activity between whole hipocampal extracts and synaptoneurosomes that we detected may be explained, in part, by the fact that the synaptoneurosome-enriched fraction lacks extracellular components, in contrast to the whole hippocampus extract. Thus, it is plausible that these differences may be due to MMP-9 present in the extracellular environment, where its secretion and subsequent activation by processing may be triggered in response to enhanced neuronal activity.

To evaluate changes more locally, we then used *in situ* zymography of brain sections, an experimental approach that detects net protease activities (but not inactive pro-enzyme and enzyme–endogenous inhibitor complexes) through the dequenched fluorescein signal from cleaved fluorescein-conjugated gelatin.[44] In control animals, we detected the highest fluorescence in the *stratum pyramidale* of CA1 and the granule cell layer of dentate gyrus (Figure 5A,G), i.e., in areas of high cell density. Because of technical limitations of epifluorescent microscopy, we were unable to specify whether the gelatinase activity was located in the cytoplasm and/or nuclei. On the other hand, we detected the lowest gelatinolytic activity in the *stratum radiatum* (28% vs *stratum pyramidale*) and the molecular layer (21% vs the granule cell layer) (Figure 5A,G).

The effects of stress and recovery period on gelatinase activity are displayed in panels B and C and panels H and I of Figure 5, respectively. Kruskall–Wallis analysis of quantitative data revealed the effect of treatments on the *stratum pyramidale* (P = 0.0038) and granule cell layer (P = 0.0025). Postanalysis indicated a significant increase in gelatinase activity in the *stratum pyramidale* (P = 0.0084) and the granule cell layer (P = 0.0067) during the stress recovery period in comparison to the level during stress (Figure 5, bottom panel). As in the somatic cell layer, we detected an increase in gelatinolytic activity in the *stratum radiatum* and the molecular layer, and the Kruskal–Wallis test indicated a significant effect of the procedure (P = 0.0388 and P < 0.0001, respectively). Dunn's post hoc analysis indicated a significant increase in gelatinolytic activity 24 h after stress in the *stratum radiatum* and molecular layer (Figure 5, bottom panel; P = 0.0420 and P = 0.0017, respectively).

To gain some insight with respect to the type of protease that was activated, we used a MMP inhibitor, CAS 1177749-58-4 (IC_{50} values of 5 nM for MMP-9, 113 nM for MMP-13, and 1050 nM for MMP-1 reported *in vitro*[54]), that has been previously used in a chronic stress model that evaluated MMP-9 activity in the hippocampus.[29] The increase in gelatinolytic activity observed 24 h after the stress procedure in both somatic and synaptic layers (compare panels C and F of Figure 5 and panels I and L of Figure 5) was blocked by 250 nM MMP inhibitor. A similar prevention was observed using 0.3 mM PMSF, a serine-protease inhibitor, in the presence of cation chelator 1 mM EDTA (Figure S4).

In our study, the changes in gelatinase activity observed during the stress recovery period in somatic and synaptic layers were sensitive to PMSF/EDTA and 250 nM MMP inhibitor that is expected to inhibit mostly the activity of MMP-9 and partially the activity of MMP-13. Furthermore, considering that gelatin is not the preferred MMP-13 substrate,[55] we inferred that MMP activity that increased 24 h after a single stress session is related to MMP-9. In addition, we must note that the activity detected by *in situ* zymography corresponds to the active form of the enzyme. It is well-known that MMP-9 is released in its latent form and activated extracellularly,[56] and in our model, it is possible that stress-induced neuronal activity may favor the release and processing of MMP-9. Therefore, gelatinolytic activity insensitive to enzyme inhibitors (MMP-9 inhibitor I and PMSF/EDTA) could correspond to other gelatinases that, in part, are activated during tissue processing for *in situ* zymography.

We highlight the fact that MMP-9 and MMP-2 have different responses in terms of their protein levels and distribution profiles in cellular and synaptic compartments. Net MMP activity, its sensitivity to MMP inhibitor, and the rise in MMP-9 protein levels at synaptoneurosomes are findings that occur during the stress recovery period, allowing us to postulate that stress triggers a delayed response, inducing an increase in MMP-9-dependent gelatinolytic activity. Strikingly, in synaptoneurosomes, we did not observe any processing of the *in vivo* MMP-9 substrate β-DG_{43}; in contrast, we observed an increase in its levels. In a model of autoimmune encephalomyelitis,

DOI: 10.1021/acschemneuro.7b00387
ACS Chem. Neurosci. 2018, 9, 945–956

interestingly, some reports have shown that blood−brain barrier leukocyte infiltration involves β-DG$_{43}$ processing in brain parenchyma and seems to require MMP-9 and MMP-2 activities.[30] In our study, we observed that MMP-2 levels were reduced during the stress recovery period in whole hippocampal extracts but remained invariable at synaptoneurosomes under all experimental conditions. We do not know the functional significance of this finding, but it supports the notion that in whole extracts, MMP-9 could be, in part, responsible for β-DG$_{43}$ processing during stress.

Studies have characterized β-DG$_{43}$ as a transmembrane protein that mediates the interaction with the cytoskeleton,[57] but its role must be clarified. Nonetheless, dystroglycan KO mice show blunted LTP at CA3−CA1 hippocampal synapses elicited by high stimulation frequency, in contrast to the results for WT mice.[58] In our study, stress triggered β-DG$_{43}$ processing in whole hippocampal extracts, an effect sustained 24 h poststress. Indeed, β-DG$_{43}$ has a role not only in excitatory synapses but also as a scaffold protein at GABAergic synapses.[59] This suggests that β-DG$_{43}$ processing observed in this study may not be restricted to excitatory synapses. In mature hippocampal cultures, α-DG (α-dystroglycan) has been shown to colocalize with β-DG and GABA$_A$R clusters, but not with glutamate AMPA receptor clusters.[53] Additionally, hippocampal neurons displaying elevated synaptic activity showed increased levels of expression and exposure of α- and β-DG in the plasma membrane.[53] Moreover, the $\alpha\beta$-dystroglycan complex is necessary for the clustering of GABA$_A$Rs and has been proposed to be part of a homeostatic mechanism in response to enhanced synaptic activity.[53] Thus, in our study, the increase in β-DG$_{43}$ levels 24 h poststress at synaptic sites may correspond to a mechanism triggered to diminish neuronal excitability produced by stress.

Considering the increased activity detected by *in situ* zymography in neuronal and synaptic areas, it is possible that MMP-9 participates in the shedding of other neuronal substrates triggered by the stress response. A favored secretion of MMP-9 from the dendritic compartment may occur with enhanced glutamate neurotransmission[16] that in our model may occur under acute stress, as in other brain areas.[5,6] Thus, released MMP-9 may be rapidly activated to cleave several substrates. For instance, I-CAM-5, which is important in the regulation of elongation and maturation of dendritic spines, is cleaved by MMP-9 following NMDA receptor activation.[60] Furthermore, chronic stress triggers the cleavage of Nectin-3, a cell adhesion molecule, in a process suggested to be related to MMP-9 activity.[29] Additionally, new MMP-9 substrates have been identified by mass spectrometry in the glutamate-stimulated synaptoneurosomal fraction of the hippocampus: synaptic cell adhesion molecule-2 and collapsing response mediator protein-2.[61] Finally, we do not yet know whether MMP-9 action corresponds to a favorable or unfavorable stress response.

Summary and Conclusions. Physiologically, synaptic plasticity allows a fine-tuning of molecular modifications that prepare neurons to respond properly to environmental challenges. The adaptive stress response to external stimuli involves a myriad of mediators that modulate neuroplastic mechanisms. Here, we have described that in the hippocampus, restraint stress affects levels of MMP-9 (but not those of MMP-2), one of the most described matrix metalloproteinases in brain. This increase in MMP-9 levels was accompanied by an increase in the level of cleaved β-DG$_{43}$. Additionally, levels of MMP-9 and β-DG$_{43}$ expression were increased at synaptic zones 24 h poststress, without changes in potential enzyme activity, in the absence of β-DG$_{43}$ processing. Nonetheless, we observed enhanced net MMP-9 activity by *in situ* zymography at soma and synaptic areas, suggesting that this enzyme may degrade other substrates different from β-DG$_{43}$, which will be important to discover in future studies.

In conclusion, our data suggest that an acute psychosocial stress paradigm produces an increment in MMP-9 enzyme levels, which probably is activated extracellularly during stress recovery. Future knowledge of the neurobiological significance of these changes will be useful for understanding the impact of a single stress exposure on hippocampal functioning.

METHODS

Animals. Adult male Sprague-Dawley rats (320−350 g) derived from a stock maintained at Universidad de Chile were used. They were allowed free access to pelleted food and water and were maintained with a controlled temperature (22 °C) and a controlled photoperiod (lights on from 7:00 a.m. to 7:00 p.m.). Efforts were made to minimize both the number of animals used and their suffering. The rats were handled according to guidelines outlined and approved by the Ethical Committee of the Faculty of Chemical and Pharmaceutical Sciences, Universidad de Chile, and the Science and Technology National Commission (CONICYT), in compliance with the National Institutes of Health Guide for Care and Use of Laboratory Animals (8th ed., 2011).

Acute Stress Model. The rats were handled once per day for 7 days prior to the experimental procedures. The handling procedure consisted of picking up the rat, weighing it, and finally returning it to its home cage. The rats were randomly assigned to weight-matched groups (control and stress), and we did not use other criteria for animal grouping (such as basal state of anxiety). In this study, we used restraint stress, which was performed in a different room and consisted of placing the rats for 2.5 h in Plexiglass tubes (25 cm × 8 cm) that were wide enough to allow comfortable breathing but restricted movement (n = 18). To evaluate poststress effects, another group of animals was stressed for 2.5 h and sacrificed 24 h after the stress period (n = 20). The stress session was performed between 9:00 a.m. and 12:00 p.m. to avoid any effects associated with changes in circadian rhythms. Unstressed animals were left undisturbed in their home cage (control group; n = 20). Animals were euthanized by decapitation, and hippocampi were rapidly dissected at 4 °C, frozen under liquid N_2, and kept at −80 °C until protein levels could be determined by Western blot analyses. Furthermore, brains from another experimental group obtained by decapitation were rapidly frozen with isopentane and stored at −80 °C until the gelatinase activity in brain sections could be determined. Another group of animals was anesthetized with isofluorane [1.5% (v/v) in air] and then intracardially perfused with heparinized (2 IU/mL) saline, followed by 4% PFA/PBS, as we have previously described.[62] In these animals, it was not possible to obtain blood samples for the determination of corticosterone levels. Brains were postfixed in the same solution for 24 h and then dehydrated in 30% (p/v) sucrose/PBS. Finally, brains were rapidly frozen with isopentane and stored at −80 °C until immunofluorescence could be determined.

Serum Corticosterone Levels. Trunk blood samples were collected for the determination of serum corticosterone (CORT) levels. Special care was taken to avoid predecapitation stress during the decapitation procedure, so the other animals were left outside the room. Blood was then centrifuged at 4000g for 15 min, and serum was collected and stored at −20 °C. Hormone levels were determined using a Corticosterone ELISA Kit (Enzo, catalong no. ADI-900-097), using the instructions provided with the kit.

Isolation of the Hippocampal Extract and Synaptoneurosome-Enriched Fractions. Each hippocampus was thawed for 5 min in a homogenization buffer containing 0.35 M sucrose, 10 mM 4-(2-hydroxyethyl)-1-piperazineethanesulfonic acid (HEPES) (pH 7.4),

DOI: 10.1021/acschemneuro.7b00387
ACS Chem. Neurosci. 2018, 9, 945−956

Table 1. Primary Antibodies and Blocking Conditions Used during Western Blotting

antigen	description of immunogen	source, host species, catalog no., RRID	concentration used	primary antibody blocking solution
MMP-9	human MMP-9 amino acids 626−644	Abcam, mouse monoclonal, catalog no. ab58803, RRID AB_944235	3.3 μg/mL	4% BSA/TBS, 0.1% Tween 20
MMP-2	peptide mapping at the C-terminus of MMP-2 of human origin	Santa Cruz, goat polyclonal, catalog no. SC-6838	0.66 μg/mL	2% nonfat milk/PBS, 0.1% Tween 20
TIMP-1	NS0-derived recombinant rat TIMP-1	R&D Biosystems, goat polyclonal, catalog no. AF580, RRID AB_355455	0.3 ng/mL	3% nonfat milk/TBS, 0.1% Tween 20
β-actin	synthetic actin N-terminal amino acids DDDIAALVIDNGSGK	Sigma-Aldrich, mouse monoclonal, catalog no. A5316, RRID AB_476743	45 ng/mL	3% nonfat milk/TBS, 0.1% Tween 20
β-dystroglycan	synthetic human C-terminal amino acids PKNMTPYRSPPPYVP	Vector Laboratories, mouse monoclonal, catalog no. VP-B205, RRID AB_2336241	1:200 dilution	1.5% nonfat milk/PBS
GFAP	GFAP from pig spinal cord	Sigma-Aldrich, mouse monoclonal, catalog no. G3893, RRID AB_477010	0.1 mg/mL	1% nonfat milk/PBS, 0.1% Tween 20
LAP-2a	rat LAP2 amino acids 34−156	BD Biosciences, mouse monoclonal, catalog no. 611000, RRID AB_398313	0.5 μg/mL	3% nonfat milk/TBS, 0.1% Tween 20
synaptophysin	rat synaptophysin amino acids 205−306	BD Biosciences, mouse monoclonal, catalog no. 611880 RRID AB_399360	1.25 ng/mL	2% nonfat milk/PBS, 0.1% Tween 20
PSD-95	synthetic peptide of residues 50−150 of mouse PSD-95 conjugated to KLH	Abcam, rabbit polyclonal, catalog no. ab18258, RRID AB_444362	0.5 ng/mL	0.5% BSA/PBS

0.25 mM dithiothreitol, protease inhibitor cocktail (Roche), 0.125 mM Na_3VO_4, 2 mM NaF, and 0.25 mM sodium pyrophosphate. All procedures were conducted at 4 °C. The tissue was homogenized with a glass−Teflon homogenizer (30 strokes at 2 revolutions/segment; Heidolph motor RZR 2050 electronic). Cell debris and nuclei were removed by centrifugation at 1000*g* for 10 min. The pellet was rehomogenized and then centrifuged as described above. The pellet was resuspended in 10 mM HEPES (pH 7.4), 0.25 mM dithiothreitol, protease inhibitor cocktail (Roche), 0.125 mM Na_3VO_4, 2 mM NaF, and 0.25 mM sodium pyrophosphate and was considered as a nucleus-enriched fraction. On the other hand, the supernatants were pooled and considered as a fraction enriched with soluble and membranous components, with a low nucleus contamination level. One aliquot was taken for Western blotting analysis, and the remaining supernatant was used for the preparation of a synaptoneurosome-enriched fraction, following a described protocol,[63] with some modifications. The supernatant was passed sequentially through a series of filters, with decreasing pore sizes of 100, 80, 30, and 10 μm (Millipore, Darmstadt, Germany). The final filtrate was centrifuged at 18000*g* for 20 min at 4 °C to obtain a pellet enriched with synaptoneurosomes. Protein levels were measured by the bicinchoninic acid method, following the instructions supplied with the kit (Thermo Scientific, Rockford, IL). Finally, an aliquot of each fraction was boiled immediately in Laemmli sample buffer and stored at −80 °C until Western analysis could be performed.

Western Blot. A total of 15 or 30 μg of proteins was resolved on 10% sodium dodecyl sulfate−polyacrylamide gels and then blotted onto 0.2 μm nitrocellulose (for proteins with molecular weights of >35 kDa) or PVDF membranes (for proteins with molecular weights of <35 kDa). After several washes with TBS (Tris-buffered saline; 20 mM Tris, 150 mM NaCl, pH 7.5), membranes were blocked for 1 h and then incubated overnight at 4 °C with the desired primary antibody (see Table 1). After three rinses in TBS 0.1% Tween-20 (each lasting 5 min), blots were incubated with horseradish peroxidase (HRP)-conjugated anti-rabbit (1:10000, Thermo Scientific, Waltham, MA), HRP-conjugated anti-mouse (1:10000, 0.08 ng/μL, Thermo Scientific, catalog no. PA196831), or HRP-avidin/biotinylated anti-goat (1:1000, Vector Laboratories, Burlingame, CA) secondary antibodies at room temperature for 2 h. Membranes were then incubated with an enhanced chemiluminescent substrate (PerkinElmer Life Sciences, Boston, MA) and detected by X-ray film or a chemiluminescence imager (Syngene, Cambridge, U.K.). To obtain reliable data from Western blot analysis, we varied the time of membrane exposure to discard saturation of the β-DG_{43} signal and the same piece of membrane was exposed for a longer period of time to obtain a reliable signal over the background of the β-DG_{30} signal. Band intensities were determined and analyzed with the Un-Scan-It software (http://www.silkscientific.com; RRID SCR_013725). The levels of β-actin and PSD-95 from samples of homogenate and synaptoneurosome fractions were used to verify equivalent protein loading, respectively. We chose PSD-95 as a normalizer because β-actin levels are very low in the synaptoneurosomal fraction.

Electron Microscopy. To characterize the synaptoneurosomal fraction, an aliquot was fixed overnight with 2.5% glutaraldehyde in sodium cacodylate buffer (0.1 M, pH 7.0). The pellet was washed with the same buffer three times for 2 h. Samples were postfixed with 1% osmium tetroxide for 90 min and then washed in doubly distilled water. Samples were stained with 1% uranyl acetate for 1 h and then dehydrated in a battery of acetone, with increasing concentrations (50, 70, 95, and 100%) over 20 min. Samples were embedded in Epon resin/acetone mixture (1:1) overnight, placed in fresh pure Epon resin, and allowed to polymerize at 60 °C for 48 h. Thin sections (60 nm) obtained with an ultramicrotome (Sorvall MT5000) were stained with uranyl acetate (4% in methanol) for 2 min and finally stained with lead citrate for 5 min. Observations were performed on a Philips (Eindhoven, The Netherlands) Tecnai 12 Biotwin electron microscope at 80 kV, as we have previously described.[62]

Immunofluorescence Detection of MMP-9 and Quantitative Analysis. Coronal slices of 35 μm (bregma −2.3 to −3.8) from frozen brains[64] were obtained in a cryostat (HM500 O, Microm, Heidelberg, Germany) and then processed for immunofluorescence detection, as previously reported,[62] with some modifications. In brief, brain slices were permeabilized with 0.1% Triton X in PHEM buffer [PHEM-B, 60 mM PIPES, 25 mM HEPES, 5 mM EGTA, and 1 mM $MgCl_2$ (pH 7.2)] for 15 min and then incubated with 50 mM NH_4Cl for 5 min. After several washes, slices were incubated in a blocking solution (2% FBS, 2% BSA, and 0.2% fish gelatin in PHEM-B) for 1 h and then incubated overnight with a 1:300 dilution of the MMP-9 antibody (3.3 μg/μL, Abcam, catalog no. ab58803) in a 50% PHEM blocking solution. After three washes with PHEM-B, slices were incubated overnight at 4 °C with a 1:300 dilution of the anti-mouse fluorescent secondary antibody (Alexa-568, Molecular Probes, Invitrogen, Eugene, OR). Finally, all sections were counterstained with Hoechst 33342 (0.5 μg/mL in PBS) and mounted with DAKO fluorescent mounting medium (DAKO, Carpinteria, CA). Negative controls were obtained in the absence of a primary or secondary antibody. To quantify the variation in immunoreactivity, images were captured using a Motic EF-N Plan 40× (0.65 NA) lens in a fluorescence microscope (Motic BA 310, Epi LED FL), in which settings of exposure time and gain were adjusted using the negative control (i.e., without a primary antibody) to fix the baseline, and held constant to ensure that all images were digitized under identical resolution. Some representative images were obtained with a Zeiss (Oberkochen, Germany) LSM 700 confocal laser scanning microscope. Confocal z-stacks separated by a z-step of 2 μm were captured using a Plan-Apochromat 10× (0.3 NA) and 40× (1.4 NA) Zeiss oil immersion objective and a 0.5× digital zoom.

DOI: 10.1021/acschemneuro.7b00387
ACS Chem. Neurosci. 2018, 9, 945−956

Settings for pinhole size, aperture gain, and offset were held constant. To allow direct comparison of different data sets, imaging was performed using the same parameters for laser excitation (i.e., intensity) and photomultiplier tube gain (i.e., sensitivity) in each set of samples.

***In Situ* Zymography.** *In situ* gelatinolytic activity was assessed using a commercially available kit (EnzChek Gelatinase/Collagenase Assay Kit, Molecular Probes, Karlsruhe, Germany). Cryosections (35 μm) were slowly unfrozen and then preincubated with the reaction buffer [50 mM Tris (pH 7.4), 5 mM $CaCl_2$, and 1 μM $ZnCl_2$] for 30 min. After that, brain sections were covered with reaction buffer containing highly quenched fluorescein-conjugated gelatin (50 μg/mL) and incubated for 6 h at 37 °C in a humidified chamber. To gain insight into the gelatinolytic activities detected in brain slices, we used 250 nM MMP inhibitor CAS 1177749-58-4 (Merck) or a mix of protease inhibitors, such as PMSF (inhibitor of serine proteases, 0.3 mM) and 1 mM EDTA, which was used to inhibit calcium proteases and metalloproteases. Coronal adjacent slices were preincubated for 30 min with the inhibitors, which remained during the incubation with fluorescein-conjugated gelatin.

Sections were then fixed with 4% PFA at 4 °C for 30 min. After several washes, nuclei were stained with Hoechst as described above and finally embedded with DAKO fluorescent mounting medium (DAKO), and images were captured using a Motic EF-N Plan 10× (0.25 NA) lens in a fluorescence microscope (Motic BA 310, Epi LED FL). In this assay, cleavage of the quenched substrate by a proteinase results in an increase in fluorescein fluorescence. Sections previously fixed with 4% PFA and then incubated with the solution of fluorescein-conjugated gelatin were used as negative controls. This control was selected to adjust the background fluorescence to zero, because it includes both the fluorescence of the fixated tissue and the basal signal of DQ-gelatin. To allow direct comparison of different data sets, imaging was performed using the same parameters of laser excitation (i.e., intensity) and photomultiplier tube gain (i.e., sensitivity) for all samples.

Image Processing. All the images were processed using ImageJ (http://imagej.nih.gov/ij) tools. For immunofluorescence and *in situ* zymography quantification, several areas of the hippocampus were selected for analysis (*stratum radiatum*, *stratum pyramidale*, molecular layer, and granule cell layer). Mean fluorescence intensities were measured by one experimenter blinded to the animal condition.

Gelatin Zymography. Gelatinase activity was assessed in whole hippocampal homogenates and synaptoneurosome fractions. Briefly, protein extracts were obtained under the same conditions described above, but without DTT. Aliquots of 500 μg of proteins were added to 500 μL of gelatin Sepharose beads (GE Healthcare, catalog no. 17-0956), previously incubated with assay buffer [50 mM Tris (pH 7.5), 500 mM NaCl, 10 mM $CaCl_2$, and 0.01% Tween 20] and adjusted to a final volume of 3 mL with assay buffer. After overnight incubation with constant agitation, beads were centrifuged at 15000*g* and 4 °C and washed three times with assay buffer. Proteins were eluted from the beads by incubation with assay buffer containing 10% DMSO for 30 min at 37 °C, with constant agitation. Supernatants were recovered by centrifugation of beads and mixed with nonreducing loading buffer. Equal volumes were resolved on 10% sodium dodecyl sulfate−polyacrylamide gel electrophoresis gels containing 1 mg/mL gelatin as a substrate, and then the gel was washed four times with 2.5% Triton X-100 and incubated in developing buffer [2.5 mM Tris (pH 8.0), 200 mM NaCl, and 5 mM $CaCl_2$] for 72 h at 37 °C. The gel was fixed and stained simultaneously with 25% (v/v) isopropyl alcohol, 10% TCA, and 0.1% Coomassie Brilliant Blue R-250 and destained with 10% acetic acid and a 30% methanol solution. Images were obtained with Syngene imager (Syngene, Cambridge, U.K.). Band intensities were determined and analyzed with Un-Scan-It software (http://www.silkscientific.com; RRID SCR_013725), and results were expressed as arbitrary densitometric units relative to controls.

Statistics. Statistical analyses were performed using GraphPad Prism (GraphPad Software Inc., San Diego, CA). Data are expressed as means ± the standard error of the mean and were processed by nonparametric analysis. Differences between groups were analyzed with the Mann−Whitney U test for comparison of two groups and the Kruskal−Wallis test for comparison of three or more groups, followed by Dunn's post hoc test.

■ ASSOCIATED CONTENT

Supporting Information

The Supporting Information is available free of charge on the ACS Publications website at DOI: 10.1021/acschemneuro.7b00387.

Morphological and biochemical characterization of the synaptoneurosome fraction (Figure S1), variation in time exposure of the Western blot to detect β-DG_{43} and β-DG_{30} (Figure S2), detection of gelatinase activities by gel zymography (Figure S3), and the effect of PMSF and EDTA on the *in situ* gelatinase activity in the hippocampus (Figure S4) (PDF)

■ AUTHOR INFORMATION

Corresponding Author

*Laboratory of Neuroplasticity and Neurogenetic, Department of Biochemistry and Molecular Biology, Faculty of Chemical and Pharmaceutical Sciences, Universidad de Chile, P.O. Box 233, Santiago 1, Chile. Phone: +562-978-2923. Fax: +562-737-8920. E-mail: jfiedler@ciq.uchile.cl.

ORCID

Felipe I. Aguayo: 0000-0002-9106-598X

Jenny L. Fiedler: 0000-0002-3928-4325

Author Contributions

F.I.A. and A.A.P. contributed equally to this work. F.I.A., A.A.P., and J.L.F. designed the experiments and wrote the paper. G.J.G.-R., A.V.D., J.A.P.-B., M.T., and A.A.P. performed experiments. F.I.A., A.A.P., and P.S.R. analyzed the data. All authors edited drafts and approved the final version.

Funding

This study was supported by FONDECYT 1120528 (J.L.F.), FONDEQUIP EQM120114, and ENL025/16.

Notes

The authors declare no competing financial interest.

■ ACKNOWLEDGMENTS

The authors thank Dr. John Cidlowski and Dr. Jeff Tucker for their excellent assistance and criticism. The authors also thank Dr. Andrew Quest for providing the LAP-2a antibody, Dr. Alfonso Paredes for providing the MMP-2 antibody, and Dr. Hernán Lara for lending us his epifluorescence microscope. The authors also thank Dr. Ana María Avalos for proofreading the article.

■ REFERENCES

(1) Morris, R. G. M., Moser, E. I., Riedel, G., Martin, S. J., Sandin, J., Day, M., and O'Carroll, C. (2003) Elements of a neurobiological theory of the hippocampus: the role of activity-dependent synaptic plasticity in memory. *Philos. Trans. R. Soc., B 358*, 773−786.

(2) Chrousos, G. P. (2000) The HPA axis and the stress response. *Endocr. Res. 26*, 513−514.

(3) McEwen, B. S. (1999) Stress and hippocampal plasticity. *Annu. Rev. Neurosci. 22*, 105−122.

(4) McEwen, B. S., and Magarinos, A. M. (2001) Stress and hippocampal plasticity: implications for the pathophysiology of affective disorders. *Hum. Psychopharmacol. 16*, S7−S19.

DOI: 10.1021/acschemneuro.7b00387
ACS Chem. Neurosci. 2018, 9, 945−956

(5) Moghaddam, B., Bolinao, M. L., Stein-Behrens, B., and Sapolsky, R. (1994) Glucocorticoids mediate the stress-induced extracellular accumulation of glutamate. *Brain Res. 655*, 251−254.
(6) Popoli, M., Yan, Z., McEwen, B. S., and Sanacora, G. (2012) The stressed synapse: the impact of stress and glucocorticoids on glutamate transmission. *Nat. Rev. Neurosci. 13*, 22−37.
(7) Treccani, G., Musazzi, L., Perego, C., Milanese, M., Nava, N., Bonifacino, T., Lamanna, J., Malgaroli, A., Drago, F., Racagni, G., Nyengaard, J. R., Wegener, G., Bonanno, G., and Popoli, M. (2014) Stress and corticosterone increase the readily releasable pool of glutamate vesicles in synaptic terminals of prefrontal and frontal cortex. *Mol. Psychiatry 19*, 433−443.
(8) Jacobson, L., and Sapolsky, R. (1991) The role of the hippocampus in feedback regulation of the hypothalamic-pituitary-adrenocortical axis. *Endocr. Rev. 12*, 118−134.
(9) Joels, M., Pu, Z., Wiegert, O., Oitzl, M. S., and Krugers, H. J. (2006) Learning under stress: how does it work? *Trends Cognit. Sci. 10*, 152−158.
(10) de Quervain, D. J., Roozendaal, B., and McGaugh, J. L. (1998) Stress and glucocorticoids impair retrieval of long-term spatial memory. *Nature 394*, 787−790.
(11) Chklovskii, D. B., Mel, B. W., and Svoboda, K. (2004) Cortical rewiring and information storage. *Nature 431*, 782−788.
(12) Benson, D. L., Schnapp, L. M., Shapiro, L., and Huntley, G. W. (2000) Making memories stick: cell-adhesion molecules in synaptic plasticity. *Trends Cell Biol. 10*, 473−482.
(13) Dityatev, A., Schachner, M., and Sonderegger, P. (2010) The dual role of the extracellular matrix in synaptic plasticity and homeostasis. *Nat. Rev. Neurosci. 11*, 735−746.
(14) Wiera, G., and Mozrzymas, J. W. (2015) Extracellular proteolysis in structural and functional plasticity of mossy fiber synapses in hippocampus. *Front. Cell. Neurosci. 9*, 427.
(15) Milward, E. A., Fitzsimmons, C., Szklarczyk, A., and Conant, K. (2007) The matrix metalloproteinases and CNS plasticity: an overview. *J. Neuroimmunol. 187*, 9−19.
(16) Dziembowska, M., Milek, J., Janusz, A., Rejmak, E., Romanowska, E., Gorkiewicz, T., Tiron, A., Bramham, C. R., and Kaczmarek, L. (2012) Activity-dependent local translation of matrix metalloproteinase-9. *J. Neurosci. 32*, 14538−14547.
(17) Dziembowska, M., and Wlodarczyk, J. (2012) MMP9: a novel function in synaptic plasticity. *Int. J. Biochem. Cell Biol. 44*, 709−713.
(18) Rivera, S., Tremblay, E., Timsit, S., Canals, O., Ben-Ari, Y., and Khrestchatisky, M. (1997) Tissue inhibitor of metalloproteinases-1 (TIMP-1) is differentially induced in neurons and astrocytes after seizures: evidence for developmental, immediate early gene, and lesion response. *J. Neurosci. 17*, 4223−4235.
(19) Ganguly, K., Rejmak, E., Mikosz, M., Nikolaev, E., Knapska, E., and Kaczmarek, L. (2013) Matrix metalloproteinase (MMP) 9 transcription in mouse brain induced by fear learning. *J. Biol. Chem. 288*, 20978−20991.
(20) Nagy, V., Bozdagi, O., Matynia, A., Balcerzyk, M., Okulski, P., Dzwonek, J., Costa, R. M., Silva, A. J., Kaczmarek, L., and Huntley, G. W. (2006) Matrix metalloproteinase-9 is required for hippocampal late-phase long-term potentiation and memory. *J. Neurosci. 26*, 1923−1934.
(21) Wang, X.-b., Bozdagi, O., Nikitczuk, J. S., Zhai, Z. W., Zhou, Q., and Huntley, G. W. (2008) Extracellular proteolysis by matrix metalloproteinase-9 drives dendritic spine enlargement and long-term potentiation coordinately. *Proc. Natl. Acad. Sci. U. S. A. 105*, 19520−19525.
(22) Wiera, G., Wozniak, G., Bajor, M., Kaczmarek, L., and Mozrzymas, J. W. (2013) Maintenance of long-term potentiation in hippocampal mossy fiber-CA3 pathway requires fine-tuned MMP-9 proteolytic activity. *Hippocampus 23*, 529−543.
(23) Michaluk, P., Kolodziej, L., Mioduszewska, B., Wilczynski, G. M., Dzwonek, J., Jaworski, J., Gorecki, D. C., Ottersen, O. P., and Kaczmarek, L. (2007) Beta-dystroglycan as a target for MMP-9, in response to enhanced neuronal activity. *J. Biol. Chem. 282*, 16036−16041.
(24) Page-McCaw, A., Ewald, A. J., and Werb, Z. (2007) Matrix metalloproteinases and the regulation of tissue remodelling. *Nat. Rev. Mol. Cell Biol. 8*, 221−233.
(25) Nakamura, H., Fujii, Y., Inoki, I., Sugimoto, K., Tanzawa, K., Matsuki, H., Miura, R., Yamaguchi, Y., and Okada, Y. (2000) Brevican is degraded by matrix metalloproteinases and aggrecanase-1 (ADAMTS4) at different sites. *J. Biol. Chem. 275*, 38885−38890.
(26) Conant, K., Wang, Y., Szklarczyk, A., Dudak, A., Mattson, M. P., and Lim, S. T. (2010) Matrix metalloproteinase-dependent shedding of intercellular adhesion molecule-5 occurs with long-term potentiation. *Neuroscience 166*, 508−521.
(27) Ethell, I. M., and Ethell, D. W. (2007) Matrix metalloproteinases in brain development and remodeling: synaptic functions and targets. *J. Neurosci. Res. 85*, 2813−2823.
(28) Yamada, A., Irie, K., Deguchi-Tawarada, M., Ohtsuka, T., and Takai, Y. (2003) Nectin-dependent localization of synaptic scaffolding molecule (S-SCAM) at the puncta adherentia junctions formed between the mossy fibre terminals and the dendrites of pyramidal cells in the CA3 area of the mouse hippocampus. *Genes Cells 8*, 985−994.
(29) van der Kooij, M. A., Fantin, M., Rejmak, E., Grosse, J., Zanoletti, O., Fournier, C., Ganguly, K., Kalita, K., Kaczmarek, L., and Sandi, C. (2014) Role for MMP-9 in stress-induced downregulation of nectin-3 in hippocampal CA1 and associated behavioural alterations. *Nat. Commun. 5*, 4995.
(30) Agrawal, S., Anderson, P., Durbeej, M., van Rooijen, N., Ivars, F., Opdenakker, G., and Sorokin, L. M. (2006) Dystroglycan is selectively cleaved at the parenchymal basement membrane at sites of leukocyte extravasation in experimental autoimmune encephalomyelitis. *J. Exp. Med. 203*, 1007−1019.
(31) Moore, C. J., and Winder, S. J. (2010) Dystroglycan versatility in cell adhesion: a tale of multiple motifs. *Cell Commun. Signaling 8*, 3.
(32) Bijata, M., Wlodarczyk, J., and Figiel, I. (2015) Dystroglycan controls dendritic morphogenesis of hippocampal neurons in vitro. *Front. Cell. Neurosci. 9*, 199.
(33) Sidhu, H., Dansie, L. E., Hickmott, P. W., Ethell, D. W., and Ethell, I. M. (2014) Genetic removal of matrix metalloproteinase 9 rescues the symptoms of fragile X syndrome in a mouse model. *J. Neurosci. 34*, 9867−9879.
(34) Leuner, B., and Shors, T. J. (2013) Stress, anxiety, and dendritic spines: what are the connections? *Neuroscience 251*, 108−119.
(35) Tsigos, C., and Chrousos, G. P. (2002) Hypothalamic-pituitary-adrenal axis, neuroendocrine factors and stress. *J. Psychosom. Res. 53*, 865−871.
(36) Nakade, Y., Fukuda, H., Iwa, M., Tsukamoto, K., Yanagi, H., Yamamura, T., Mantyh, C., Pappas, T. N., and Takahashi, T. (2007) Restraint stress stimulates colonic motility via central corticotropin-releasing factor and peripheral 5-HT3 receptors in conscious rats. *Am. J. Physiol Gastrointest Liver Physiol 292*, G1037−1044.
(37) Nakade, Y., Mantyh, C., Pappas, T. N., and Takahashi, T. (2007) Fecal pellet output does not always correlate with colonic transit in response to restraint stress and corticotropin-releasing factor in rats. *J. Gastroenterol. 42*, 279−282.
(38) Hollingsworth, E. B., McNeal, E. T., Burton, J. L., Williams, R. J., Daly, J. W., and Creveling, C. R. (1985) Biochemical characterization of a filtered synaptoneurosome preparation from guinea pig cerebral cortex: cyclic adenosine 3′:5′-monophosphate-generating systems, receptors, and enzymes. *J. Neurosci. 5*, 2240−2253.
(39) Dzwonek, J., Rylski, M., and Kaczmarek, L. (2004) Matrix metalloproteinases and their endogenous inhibitors in neuronal physiology of the adult brain. *FEBS Lett. 567*, 129−135.
(40) Konopacki, F. A., Rylski, M., Wilczek, E., Amborska, R., Detka, D., Kaczmarek, L., and Wilczynski, G. M. (2007) Synaptic localization of seizure-induced matrix metalloproteinase-9 mRNA. *Neuroscience 150*, 31−39.
(41) Janusz, A., Milek, J., Perycz, M., Pacini, L., Bagni, C., Kaczmarek, L., and Dziembowska, M. (2013) The Fragile X mental retardation protein regulates matrix metalloproteinase 9 mRNA at synapses. *J. Neurosci. 33*, 18234−18241.

DOI: 10.1021/acschemneuro.7b00387
ACS Chem. Neurosci. 2018, 9, 945−956

(42) Darnell, J. C., and Klann, E. (2013) The translation of translational control by FMRP: therapeutic targets for FXS. *Nat. Neurosci. 16*, 1530−1536.
(43) Sbai, O., Ferhat, L., Bernard, A., Gueye, Y., Ould-Yahoui, A., Thiolloy, S., Charrat, E., Charton, G., Tremblay, E., Risso, J. J., Chauvin, J. P., Arsanto, J. P., Rivera, S., and Khrestchatisky, M. (2008) Vesicular trafficking and secretion of matrix metalloproteinases-2, −9 and tissue inhibitor of metalloproteinases-1 in neuronal cells. *Mol. Cell. Neurosci. 39*, 549−568.
(44) Vandooren, J., Van den Steen, P. E., and Opdenakker, G. (2013) Biochemistry and molecular biology of gelatinase B or matrix metalloproteinase-9 (MMP-9): the next decade. *Crit. Rev. Biochem. Mol. Biol. 48*, 222−272.
(45) Makowski, G. S., and Ramsby, M. L. (1998) Identification and partial characterization of three calcium- and zinc-independent gelatinases constitutively present in human circulation. *IUBMB Life 46*, 1043−1053.
(46) Kjeldsen, L., Johnsen, A. H., Sengelov, H., and Borregaard, N. (1993) Isolation and primary structure of NGAL, a novel protein associated with human neutrophil gelatinase. *J. Biol. Chem. 268*, 10425−10432.
(47) Noble, L. J., Donovan, F., Igarashi, T., Goussev, S., and Werb, Z. (2002) Matrix metalloproteinases limit functional recovery after spinal cord injury by modulation of early vascular events. *J. Neurosci. 22*, 7526−7535.
(48) Kim, Y., Remacle, A. G., Chernov, A. V., Liu, H., Shubayev, I., Lai, C., Dolkas, J., Shiryaev, S. A., Golubkov, V. S., Mizisin, A. P., Strongin, A. Y., and Shubayev, V. I. (2012) The MMP-9/TIMP-1 axis controls the status of differentiation and function of myelin-forming Schwann cells in nerve regeneration. *PLoS One 7*, e33664.
(49) Vandooren, J., Born, B., Solomonov, I., Zajac, E., Saldova, R., Senske, M., Ugarte-Berzal, E., Martens, E., Van den Steen, P. E., Van Damme, J., Garcia-Pardo, A., Froeyen, M., Deryugina, E. I., Quigley, J. P., Moestrup, S. K., Rudd, P. M., Sagi, I., and Opdenakker, G. (2015) Circular trimers of gelatinase B/matrix metalloproteinase-9 constitute a distinct population of functional enzyme molecules differentially regulated by tissue inhibitor of metalloproteinases-1. *Biochem. J. 465*, 259−270.
(50) Malla, N., Sjoli, S., Winberg, J. O., Hadler-Olsen, E., and Uhlin-Hansen, L. (2008) Biological and pathobiological functions of gelatinase dimers and complexes. *Connect. Tissue Res. 49*, 180−184.
(51) Smalheiser, N. R., and Collins, B. J. (2000) Coordinate enrichment of cranin (dystroglycan) subunits in synaptic membranes of sheep brain. *Brain Res. 887*, 469−471.
(52) Zaccaria, M. L., Di Tommaso, F., Brancaccio, A., Paggi, P., and Petrucci, T. C. (2001) Dystroglycan distribution in adult mouse brain: a light and electron microscopy study. *Neuroscience 104*, 311−324.
(53) Pribiag, H., Peng, H., Shah, W. A., Stellwagen, D., and Carbonetto, S. (2014) Dystroglycan mediates homeostatic synaptic plasticity at GABAergic synapses. *Proc. Natl. Acad. Sci. U. S. A. 111*, 6810−6815.
(54) Levin, J. I., Chen, J., Du, M., Hogan, M., Kincaid, S., Nelson, F. C., Venkatesan, A. M., Wehr, T., Zask, A., DiJoseph, J., Killar, L. M., Skala, S., Sung, A., Sharr, M., Roth, C., Jin, G., Cowling, R., Mohler, K. M., Black, R. A., March, C. J., and Skotnicki, J. S. (2001) The discovery of anthranilic acid-based MMP inhibitors. Part 2: SAR of the 5-position and P1(1) groups. *Bioorg. Med. Chem. Lett. 11*, 2189−2192.
(55) Snoek-van Beurden, P. A., and Von den Hoff, J. W. (2005) Zymographic techniques for the analysis of matrix metalloproteinases and their inhibitors. *BioTechniques 38*, 73−83.
(56) Van den Steen, P. E., Dubois, B., Nelissen, I., Rudd, P. M., Dwek, R. A., and Opdenakker, G. (2002) Biochemistry and molecular biology of gelatinase B or matrix metalloproteinase-9 (MMP-9). *Crit. Rev. Biochem. Mol. Biol. 37*, 375−536.
(57) Barresi, R., and Campbell, K. P. (2006) Dystroglycan: from biosynthesis to pathogenesis of human disease. *J. Cell Sci. 119*, 199−207.
(58) Moore, S. A., Saito, F., Chen, J., Michele, D. E., Henry, M. D., Messing, A., Cohn, R. D., Ross-Barta, S. E., Westra, S., Williamson, R. A., Hoshi, T., and Campbell, K. P. (2002) Deletion of brain dystroglycan recapitulates aspects of congenital muscular dystrophy. *Nature 418*, 422−425.
(59) Lévi, S., Grady, R. M., Henry, M. D., Campbell, K. P., Sanes, J. R., and Craig, A. M. (2002) Dystroglycan is selectively associated with inhibitory GABAergic synapses but is dispensable for their differentiation. *J. Neurosci. 22*, 4274−4285.
(60) Tian, L., Stefanidakis, M., Ning, L., Van Lint, P., Nyman-Huttunen, H., Libert, C., Itohara, S., Mishina, M., Rauvala, H., and Gahmberg, C. G. (2007) Activation of NMDA receptors promotes dendritic spine development through MMP-mediated ICAM-5 cleavage. *J. Cell Biol. 178*, 687−700.
(61) Bajor, M., Michaluk, P., Gulyassy, P., Kekesi, A. K., Juhasz, G., and Kaczmarek, L. (2012) Synaptic cell adhesion molecule-2 and collapsin response mediator protein-2 are novel members of the matrix metalloproteinase-9 degradome. *J. Neurochem. 122*, 775−788.
(62) Pacheco, A., Aguayo, F. I., Aliaga, E., Munoz, M., Garcia-Rojo, G., Olave, F. A., Parra-Fiedler, N. A., Garcia-Perez, A., Tejos-Bravo, M., Rojas, P. S., Parra, C. S., and Fiedler, J. L. (2017) Chronic Stress Triggers Expression of Immediate Early Genes and Differentially Affects the Expression of AMPA and NMDA Subunits in Dorsal and Ventral Hippocampus of Rats. *Front. Mol. Neurosci. 10*, 244.
(63) Williams, C., Mehrian Shai, R., Wu, Y., Hsu, Y.-H., Sitzer, T., Spann, B., McCleary, C., Mo, Y., and Miller, C. A. (2009) Transcriptome analysis of synaptoneurosomes identifies neuroplasticity genes overexpressed in incipient Alzheimer's disease. *PLoS One 4*, e4936.
(64) Paxinos, G., and Watson, C. (1982) *The Rat Brain in Stereotaxic Coordinates*, 7th ed., Academic Press.

DOI: 10.1021/acschemneuro.7b00387
ACS Chem. Neurosci. 2018, 9, 945−956